

PROFILE-FOLLOWING ENTRY GUIDANCE USING LINEAR QUADRATIC REGULATOR THEORY

Invited (John Hanson)-session #1

Greg A. Dukeman¹
NASA Marshall Space Flight Center
Huntsville, AL 35812

gains are more or less trajectory-independent which is a potentially useful property.

Abstract

This paper describes one of the entry guidance concepts that is currently being tested as part of Marshall Space Flight Center's Advance Guidance and Control Project. The algorithm is of the reference profile tracking type. The reference profile consists of the reference states, range-to-go, altitude, and flight path angle, and reference controls, bank angle and angle of attack, versus energy. A linear control law using state feedback is used with energy-scheduled gains. The gains are obtained offline using Matlab's steady state linear quadratic regulator function. Lateral trajectory control is effected by performing periodic bank sign reversals based on a heading error corridor. A description and results of the AG&C test cases on which it has been tested are given. Although it is not anticipated that the algorithm will be quite as robust as algorithms with onboard trajectory re-generation capability, the results nevertheless show it to be very robust with respect to varying initial conditions and works satisfactorily even for entries from widely different orbits than that of the reference profile. Moreover, the commanded bank and angle of attack histories are very smooth, making it easier for the attitude control system to implement the guidance commands. Finally, results indicate that the guidance

NOTATION

AG&C	Advanced Guidance and Control
Project	
EAEB	Edwards Air Force Base
GRAM95	Global Reference Atmospheric
Model - 1995	
HAC	Heading Alignment Cylinder
MAAF	Michael Army Air Field
MECO	Main Engine Cutoff
POST	Program to Optimize Simulated
Trajectories	
Q-alpha	product of dynamic pressure and
angle of attack	
RLV	Reusable Launch Vehicle
TAEM	Terminal Area Energy
Management	
C_L	lift coefficient
C_D	drag coefficient
e	vehicle energy
g	gravitational acceleration, 32.2
ft/s^2	
h	altitude
r	Earth center to vehicle position
vector magnitude	
R	range
R_{nom}	nominal range-to-go
R_{req}	required range-to-go

¹ Guidance and Navigation Specialist, Vehicle Flight Mechanics Group

s	great circle range from vehicle to
target point	
u	inplane component of L/D or L/D
$\cos(\sigma)$	
v	Earth relative velocity vector
magnitude	
z	drag profile tracking error, $D_{est} -$
D_{ref}	
α_{cmd}	commanded angle of attack
α_{ei}	entry interface angle of attack
α_{nav}	estimated angle of attack from
navigation system	
β	inverse scale height in
exponential density model	
γ	relative flight path angle
ϕ	latitude
ρ	atmospheric density
σ_{cmd}	commanded bank angle
σ_{ei}	entry interface bank angle
σ_{nav}	estimated bank angle from
navigation system	
ψ	heading of relative velocity
vector from local north	
ψ_d	desired heading of relative
velocity vector	
ω	Earth rotation rate

Introduction

The objective of NASA's Second Generation Reusable Launch Vehicle (RLV) program is to reduce the cost of putting a pound of payload into orbit from \$10,000 to \$1,000 and to increase safety from 1 catastrophic failure in 100 flights to 1 in 10,000. Several key technology areas, including airframes, propulsion, flight demonstrations, flight mechanics, integrated vehicle health management, operations, and vehicle subsystems, are being studied to help meet these ambitious goals. Within the flight mechanics area, advanced guidance and control algorithms featuring a high degree of robustness and autonomy are being developed by government, industry, and academic researchers. Marshall Space Flight Center's Advanced Guidance and Control Project was created to provide realistic and objective test procedures and scenarios to evaluate promising algorithms. This paper describes and gives results for one of the entry guidance algorithms currently undergoing testing as part of the AG&C project.

This paper begins with a description of the entry guidance problem, followed by development of the algorithm formulation. Next, the AG&C entry guidance test cases are discussed followed by Monte Carlo

simulation results. The paper ends with conclusions and recommendations.

Entry Guidance Problem Description

The problem under consideration is that of an unpowered lifting vehicle re-entering the atmosphere.* It is assumed that the vehicle is actively controlled so that the angle of attack and/or angle of bank can be modulated, thus effecting trajectory control via lift and drag modulation. The reentry trajectories being examined correspond to both space shuttle type re-entry from Low-Earth Orbit and to low-speed (speeds significantly below orbital speeds) re-entry consistent with a sub-orbital flight demonstrator like X-33, X-34, or X-37. The entry guidance is responsible for controlling the trajectory from entry interface (defined roughly as 1) 400kft altitude for reentry from LEO or 2) several seconds after the powered phase for sub-orbital reentry) until the vehicle's Earth-relative speed has reduced to a value commensurate with handover to TAEM guidance, typically 3,000 fps at 90,000 feet altitude and between 30 and 60 nautical miles from the landing site. commanding the aerodynamic angles, bank and angle of attack

The guidance algorithms must be flexible enough to accommodate these various profiles and to adapt to severe off-nominal dispersions, such as early engine failure (partial or total) where possibly more than half the thrust is lost.

The X-33 trajectory profile is conveniently divided into five flight phases: 1) ascent, 2) transition, 3) entry, 4) Terminal Area Energy Management (TAEM), 5) Approach and Landing (A/L) and are defined as follows.

The transition phase is defined as the period from Main Engine Cut Off (MECO) until a specified minimum time has elapsed and the sensed aerodynamic accelerations have exceeded some threshold value and the vehicle is descending. The purpose of the transition phase is to maneuver to a specified entry interface attitude and hold until sufficient aerodynamic force

* Although this paper gives results for Earth entry only, the algorithm formulation is not inherently restricted to a particular atmosphere or planet.

exists to provide entry trajectory control via bank angle modulation.

Note that the ascent phase is followed very shortly, after just several seconds, by the entry phase. This results in bigger entry condition dispersions than those associated with a reentering orbital vehicle wherein an exoatmospheric deorbit burn places the vehicle on an entry path. Off-nominal X-33 ascent profiles result in off-nominal entry conditions that the entry guidance must be robust enough to handle.

GUIDANCE ALGORITHM FORMULATION

The transition guidance algorithm is fairly simple. Desired entry interface attitude is specified via the mission design loads $\alpha_{TransitionDeg}$, and $\phi_{ibkTransitionDeg}$ representing desired angle of attack and velocity bank angle magnitude. The appropriate bank sign to use is computed at transition initiation and is a simple function of the MECO velocity heading and the desired velocity heading (refer to Notation section)

$$\text{sgn}(\sigma_{cmd}) = -\text{sgn}(\psi - \psi_d) \quad (1)$$

See Figure 5 for definitions of heading angles. The bank sign thus computed is used throughout transition and subsequently used to initialize entry guidance bank command sign. In order to provide smooth bank and angle of attack commands, the output σ_{cmd} of the filter represented by the following equation is passed as bank command to the attitude control system

$$\ddot{\sigma}_{cmd} + 2\zeta\omega_n\dot{\sigma}_{cmd} + \omega_n^2(\sigma_{cmd} - \sigma_{ei}) = 0 \quad (2)$$

and analogously for angle of attack

$$\ddot{\alpha}_{cmd} + 2\zeta\omega_n\dot{\alpha}_{cmd} + \omega_n^2(\alpha_{cmd} - \alpha_{ei}) = 0 \quad (3)$$

The filter states α_{cmd} and σ_{cmd} are initialized during the first pass through transition guidance by setting the commanded values equal to the current estimated bank and angle of attack provided by the navigation subsystem and zeroing the filter rates

$$\alpha_{cmd} = \alpha_{nav}, \sigma_{cmd} = \sigma_{nav}, \dot{\alpha}_{cmd} = 0, \dot{\sigma}_{cmd} = 0 \quad (4)$$

(initialization)

Commanded bank and angle of attack rates are generated, not by using the filter rates, but by comparing commanded angles with estimated angles.

$$\dot{\alpha}_{cmd} = (\alpha_{cmd} - \alpha_{nav})/2, \quad \dot{\sigma}_{cmd} = (\sigma_{cmd} - \sigma_{nav})/2 \quad (5)$$

These rates are limited before being sent to the attitude control system

$$|\dot{\alpha}_{cmd}| \leq \dot{\alpha}_{\max, transition}, \quad |\dot{\sigma}_{cmd}| \leq \dot{\sigma}_{\max, transition} \quad (6)$$

Entry Guidance

The guidance algorithm controls range to a specified landing site by issuing bank angle commands which will cause the reentry vehicle to track a nominal profile consisting of range-to-go, altitude, flight path versus relative energy profile. The profile is a by-product of the overall (ascent through entry) trajectory design process, using the Program to Optimize Simulated Trajectories (POST). All relevant constraints such as range, heating and dynamic pressure limits are enforced in the trajectory design process. This ensures that when the reentry vehicle flies the resulting nominal drag profile, all relevant entry constraints are satisfied. Lateral trajectory control is provided via bank reversal logic which is described later. Entry guidance is terminated at an Earth-relative velocity of 3,000 ft/s.

This section is organized as follows. First, range (longitudinal) control equations and logic are developed. Then, synthesis of a linear tracking control law is discussed in which bank angle modulation is used to follow a reference profile. Next, heading (lateral) control equations are discussed.

Range Control The basic idea is to develop a nominal profile which can be tracked by the vehicle via bank angle modulation. For guidance purposes, the relevant equations of motion are those corresponding to planar motion about a non rotating Earth, with central gravity and aerodynamic lift and drag forces³

$$\begin{aligned}
\dot{R} &= v \cos \gamma \\
\dot{r} &= v \sin \gamma \\
\dot{v} &= -D - g \sin \gamma \\
v\dot{\gamma} &= \left(\frac{v^2}{r} - g \right) \cos \gamma + Du
\end{aligned}
\tag{7}$$

where the control u is the vertical or in-plane component of lift to drag ratio

(8)

The horizontal distance (range) corresponding to flight along a drag-energy profile can be computed as follows. Define relative energy

$$e = v^2 / 2 + gh \tag{9}$$

and the time rate of change of energy is

$$\dot{e} = v\dot{v} + \dot{g}h + g\dot{h} \cong v(-D - g \sin \gamma) + gv \sin \gamma = -Dv \tag{10}$$

The time rate of change of range R is given by

(11)

for near zero flight path angle (greater than about -5 degrees). Note that the restriction on flight path angle, i.e., small magnitude, implies that the valid region of reentry for drag-energy guidance extends down to about Mach 2.5, where typically flight path angle starts becoming large negative. Figure 6 shows a typical drag-energy profile.

Tracking Control Law Synthesis In the following, the technique of feedback linearization is used to obtain an adaptive linear tracking control law. Throughout the derivation of the control law, assume an exponential atmosphere model of the form

$$\rho(h) = \rho_0 \exp(-\beta h) \tag{13}$$

and use the approximation that time rate of change of drag coefficient is zero. (It is not difficult to remove the latter assumption and doing so does not appreciably complicate the control law.)

The control law depends upon the current state (r, v, γ), the drag-energy profile, the inverse scale height, β , the estimated current drag acceleration and the design parameters ω and damping ratio, ζ . Note that the control law is independent of the current density and the current lift and drag coefficients. The estimated drag is just the component of sensed acceleration along the current navigated relative velocity vector. The sensed acceleration is equal to the accumulated velocity counts from the navigation system over the last one second.

$$R_{req} = \frac{s\Psi_e}{\sin(\Psi_e)}$$

(22)

where Ψ_e is the current heading error. The cyclically calculated values from (21) are the values of reference drag and slope that are used in the control law.

Angle of attack is nominally commanded according to a pre-specified Mach-alpha schedule. Figure 7 shows a typical angle of attack profile. To augment bank angle control, angle of attack modulation about the nominal schedule is used. This value is passed through a limiter to keep commanded angle of attack within five degrees of the nominal schedule. This alpha modulation capability is particularly useful during roll reversals and during short-period transients.

The bank command is limited to between 0 and 85 degrees so that when a roll reversal is commanded, smaller maneuvers are required. The sign of the bank command is determined from the logic of the next section. Finally, to ensure that bank and angle of attack commands are reasonably consistent with vehicle attitude maneuver limitations, these two quantities are passed through a function that models the bank and angle of attack dynamics as second order systems with pre-specified rate and acceleration limits. This is analogous to the Transition Guidance logic. As in

transition guidance, outputs to the control system are again bank, bank rate, alpha, and alpha rate.

Heading Angle Control The lateral logic is, for the most part, uncoupled from the longitudinal (range) control. During reentry, the lateral logic determines the sign of the commanded bank angle and does it independently of the range control (which determines the appropriate magnitude of the bank angle command).

In Ref. 6, a heading error versus speed corridor is stored onboard to determine when to command roll reversals. To minimize the extent to which the heading error corridor is tied to a specific entry profile, a new, more general approach has been developed for X33 reentry lateral control, a description of which follows.

The time rate of change of velocity heading angle is written³

$$\dot{\psi} = -\frac{L \sin(\sigma)}{v \cos(\gamma)} + \frac{v}{r} \cos(\gamma) \sin(\psi) \tan(\phi) - 2\omega(\tan(\gamma) \cos(\psi) \cos(\phi) - \sin(\phi)) \quad (27)$$

Likewise, an expression for the time rate of change of desired heading (omitted here for brevity) can be obtained from its definition so that the time rate of change of heading error is

$$\dot{\psi}_e = \dot{\psi}_d - \dot{\psi} = \dot{\psi}_d - \frac{L \sin(\sigma)}{v \cos(\gamma)} + \frac{v}{r} \cos(\gamma) \sin(\psi) \tan(\phi) - 2\omega(\tan(\gamma) \cos(\psi) \cos(\phi) - \sin(\phi)) \quad (28)$$

Equating to zero, and solving for bank angle gives

$$\sin(\sigma) = \dot{\psi}_d + \frac{v^2}{Lr} \cos^2(\gamma) \sin(\psi) \tan(\phi) - 2\omega \frac{v \cos(\gamma)}{L} \sin(\tan(\gamma) \cos(\psi) \cos(\phi) - \sin(\phi)) \quad (29)$$

This value is the bank angle required to maintain the current heading error. If the magnitude of the required bank is greater than 12 degrees, then a sign change (on the commanded bank angle) is indicated.

Vehicle Description

The X-33 vehicle is a vertically launched, single stage lifting body vehicle powered by two linear

aerospike engines burning liquid oxygen and liquid hydrogen.

NOMINAL MISSION PROFILE

The first flight will be a benign low-speed (maximum Mach = 8) flight to Michael Army Air Field. Subsequent flights will have as objectives maximum entry catalytic heating, maximum entry integrated heat load, maximum delay of transition to turbulent flow, and attainment of desired vehicle surface temperatures. Figures 8 through 15 show trajectory parameters of interest for the maximum catalytic heating mission.

Figure 13 Nominal Angle of Attack History

Figure 14 Nominal Dynamic Pressure and Q-alpha History

Simulation Results

A Monte Carlo analysis was performed to test the robustness of the guidance algorithm to propulsion, atmospheric, navigation, and aerodynamic uncertainties. Propulsion system uncertainties include +/- 1 percent Isp, propellant utilization uncertainties, 404.1 lbm loaded LOX uncertainty, 54.96 lbm loaded LH2 uncertainty. Atmospheric uncertainties are modeled using GRAM9510 for density and entry wind uncertainties, and several dozen measured wind data sets for ascent wind uncertainties. Three degree-of-freedom simulations were made from launch to the entry/TAEM handover point - 3,000 ft/s Earth-relative velocity.

Conclusions

This paper describes an entry guidance algorithm that is currently undergoing testing in MSFC's Advanced Guidance and Control Project. The robustness of the algorithms in the presence of navigation, atmospheric, aerodynamics, and propulsion system uncertainties.

Conclusions

Acknowledgement

References

2. Roenneke, Axel, and Markl, Albert, "Reentry Control to a Drag-Energy Profile", Journal of Guidance,

Control and Dynamics, Vol. 17, No. 5, Sept. - Oct. 1994.

3. Vinh, Nguyen, Optimal Trajectories in Atmospheric Flight, Chapter 3, Elsevier Scientific Publishing Company, 1981.

4. Tannas, Lawrence E. Jr., and Perkins, Toney R., "Simulation Evaluation of Closed Form Reentry Guidance", AIAA Guidance, Control and Flight Dynamics Conference, 1967, AIAA Paper 67-597.

6. Harpold, Jon C., and Graves, Claude A. Jr., "Shuttle Entry Guidance", Journal of the Astronautical Sciences", Vol. XXVII, No. 3, pp. 239-268, July-September, 1979.

7. Lu, Ping, "Entry Guidance and Trajectory Control for Reusable Launch Vehicle", Journal of Guidance, Control and Dynamics, Vol. 20, No. 1, January-February, 1997, pp. 143-149.

8. Mease, Kenneth M., and Kremer, Jean-Paul, "Shuttle Entry Guidance Revisited Using Nonlinear Geometric Methods", Journal of Guidance, Control, and Dynamics, Vol. 17, No. 6, 1994, pp. 1350-1356.

10. Justus, C.G., Jeffries, W.R. III, Yung, S.P., and Johnson, D.L., "The NASA/MSFC Global Reference Atmospheric Model-1995 Version (GRAM-95)", NASA Technical Memorandum 4715, August 1995.

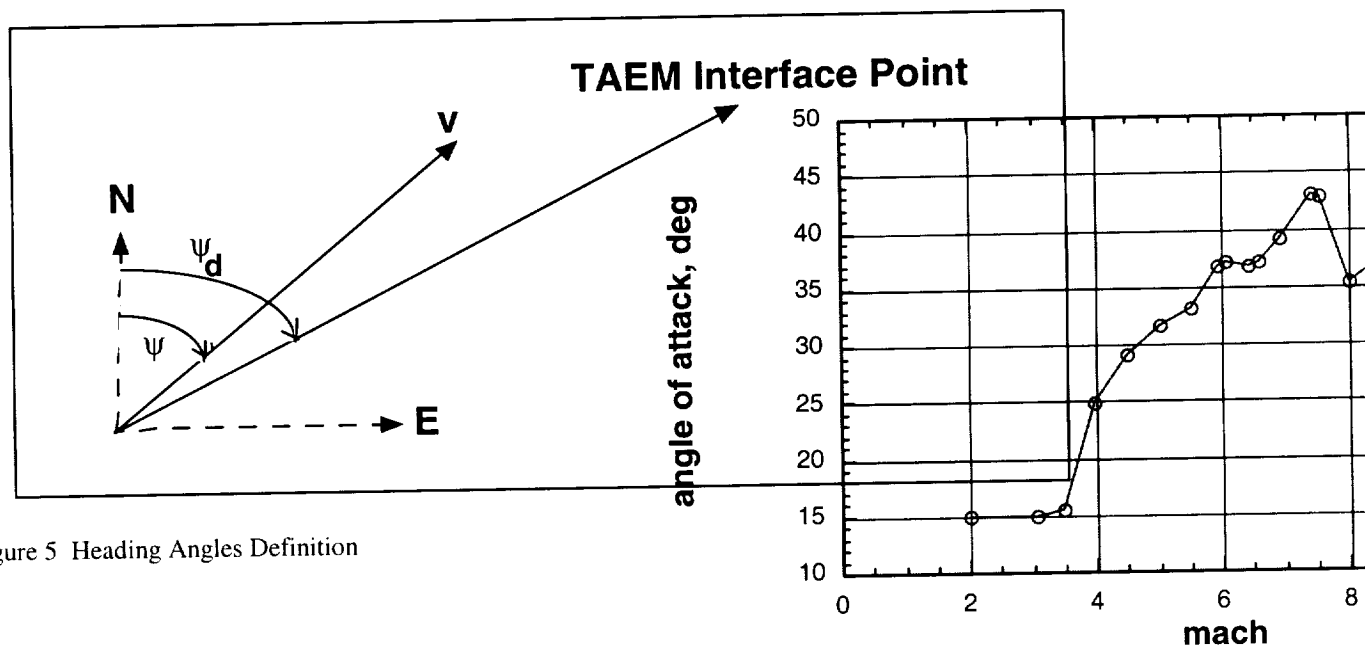


Figure 5 Heading Angles Definition

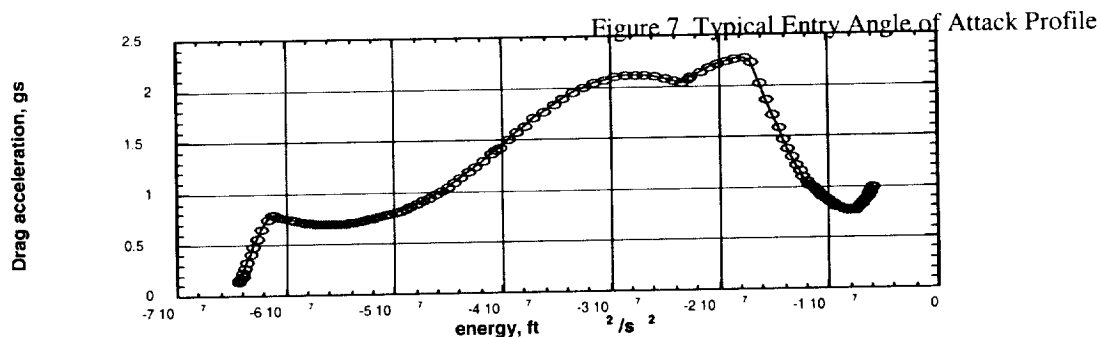


Figure 6 Typical Drag-Energy Profile

Energy Profile

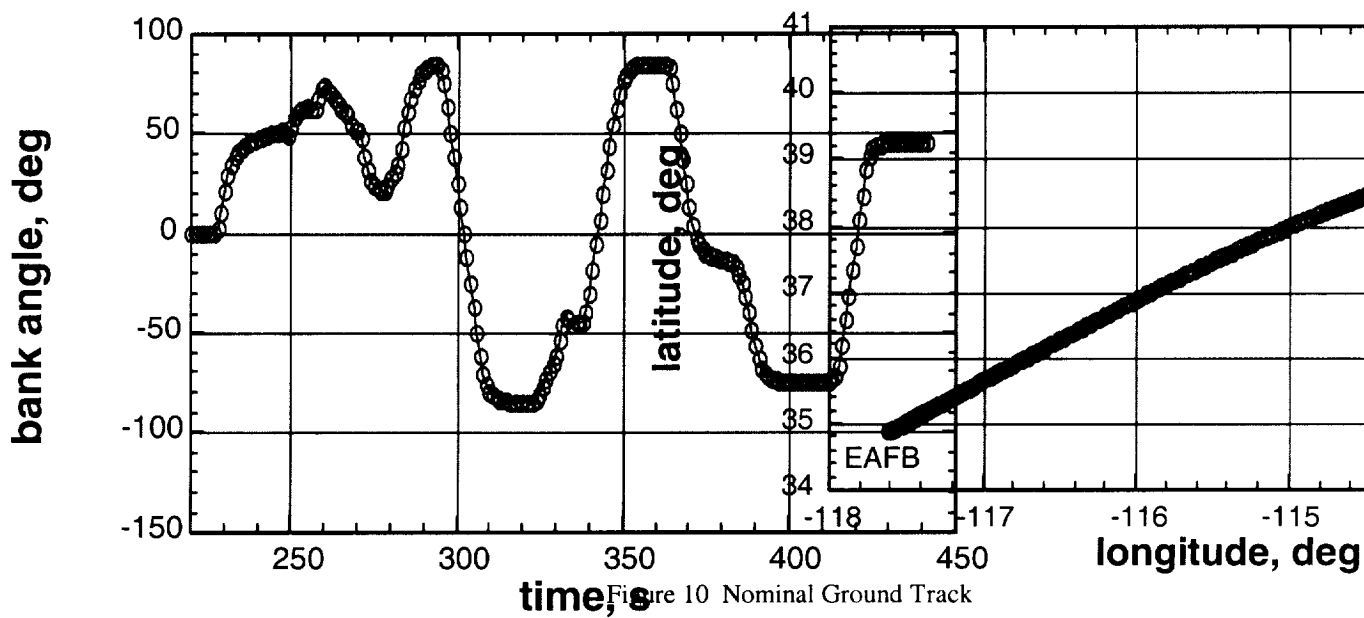


Figure 11 Nominal Entry Bank Angle History

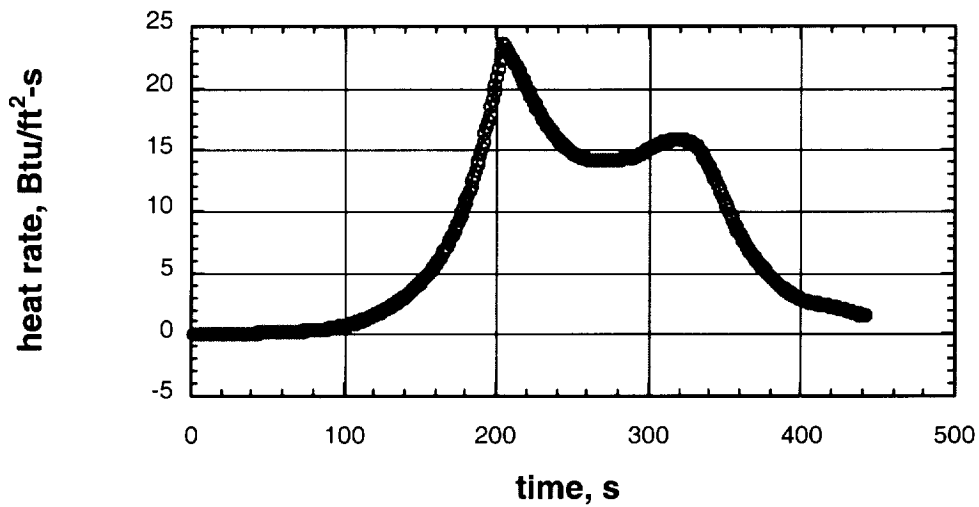


Figure 15 Nominal Heat Rate History